

Comparative Analysis of the Vibrational Response of Different Main Rotor Blades of a Homemade Helicopter

Julius Kewir Tangka

Renewable Energy Laboratory, Department of Agricultural Engineering, FASA, University of Dschang, Cameroon.
E.mail tangkajkfr@juliustangka.org

John Ngangsi Ngah

Renewable Energy Laboratory, Department of Agricultural Engineering, FASA, University of Dschang, Cameroon

Godlove Suila Kuaban

Institute of Theoretical and Applied Informatics, Polish Academy of Sciences
Baltycka 5, 44-100 Gliwice Poland

Mathias N. W. Evina

Renewable Energy Laboratory, Department of Agricultural Engineering, FASA, University of Dschang, Cameroon

ABSTRACT

This paper investigates the dynamics of homemade helicopter wooden and aluminum sheet rotor blades. The rotors are articulated and their blades are rigid. The main rotor implementation takes into account flap, lag, and feather degrees of freedom for each of the equispaced blades as well as their dynamic couplings. Transmitted vibrations due to the rotating rotor blades on the body structure (fuselage) are studied. This work presents an aerodynamic model of main rotor blades that allows us to analyse vibrational transmissions on the fuselage (body) of the craft. Vibrations in helicopters are a common problem which involves complex interactions between the inertial, structural and aerodynamic loads, especially in homemade helicopters. The major source of vibrations in helicopters is the main rotor. The efficiency and stability of the main rotor blades is determined by the magnitudes of the predominant frequencies they produce. These vibrations affect the functionality, durability of the engine component parts, increase maintenance frequency (cost), and cause structural failures. The aerodynamic model has been built up using blade element theory. The aerodynamic load creates vibrations on the homemade helicopter and these are analyzed on the fuselage by using a short time Fourier transform that brings out the vibrational spectrum. The results of the analysis serve as a reference to characterize the stability and efficiency of homemade main rotor blade profiles.

Keywords: Vibrations, propellers, homemade helicopter, blade profiles, aerodynamics.

INTRODUCTION

In helicopters, and similar flying machines the main rotor blades vibrations are a common problem which involve complex interactions between the inertial, structural, and aerodynamic loads. The major source of vibrations in the main rotor blades is the unbalanced masses of the blades or out of track alignment. In aircraft's design, vibrations have remained one of the major problems affecting helicopter development for years. In fact, the maximum speed and maneuvering capabilities for most modern helicopters are limited by excessive vibration. Vibration frequencies are either equal to the rotor frequencies or multiples of them. The rotor frequencies are a function of the angular speeds at which they rotate [1]. Vibrations affect the functionality of the engine component parts, increase maintenance frequency and cost, affect passenger comfort and fatigue otherwise known as ergonomics, and sometimes cause structural failures. High vibration levels experienced by a helicopter could, in many cases, pose a limitation to the vehicle's maneuvering capabilities and forward speed. In addition to this, vibrations affect the helicopter handling qualities, contribute to the fatigue of structural components, reduce the reliability of the main frame design and on-board electronic equipment, and influence the precision of equipment such as cameras, measuring devices, etc. [2], [3]. As a result, reducing helicopter vibrations has traditionally been a difficult task. It is important to study and analyze vibrations in order to identify the predominant frequencies responsible for the vibrations. This results can be used to determine the most performant main rotor blade profile [4]. In this work, the vibrations generated by the main rotors and transmitted to the fuselage are detected using vibration sensors and an accelerometer. The data, which is the displacement in the x and y axes, is collected and processed using matlab software. The result, which is a vibration spectrum, will enable us to identify the predominant frequencies. These predominant frequencies will be used as specific reference to characterize the stability and efficiency of homemade main rotor blades. The structure of the article is as follows: in sections 2 and 3, the aspects of the dynamic helicopter model are considered. In section 4, the aerodynamic model is provided. Vibrational analysis on the fuselage, as a consequence of the aerodynamic and dynamic loads are given in Section 5. Section 6 contains the conclusions of the article.

DYNAMIC MODEL

The helicopter's main rotor blades are perpendicular to those of the tail rotor. Both systems are mounted on the fuselage. The helicopter model consists of a fuselage, a main rotor, and a tail rotor, both articulated, (figure 1). The main rotor consists of two equally spaced blades joined to a central hub, and the tail rotor consists of two equally spaced blades joined to a secondary hub. The blades are rigid in both rotors. The helicopter has six degrees of freedom: three translations along the (X, Y, and Z) axes and three rotations around the same axes. The model presented in this paper is based on previous work by some authors, ([5, 6, 7, 8, and 9]).

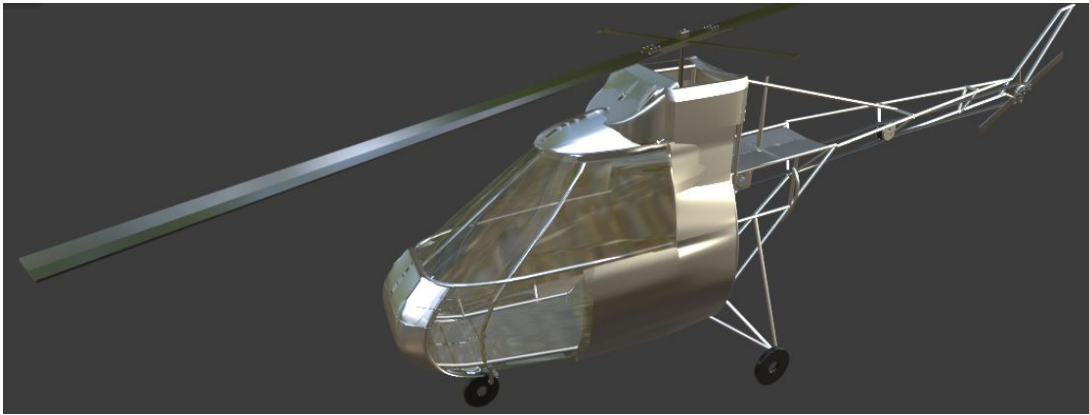


Figure 1: The homemade helicopter concept model

Fuselage

The fuselage is the main body section that holds rotorcraft's engine, crew, and amongst others. It has three degrees of freedom: lateral and longitudinal translation in the horizontal plane (X-Y axis), vertical translation (Z axis), and rotation about these same axes (pitch, roll, and yaw).

Main rotor

Design of wooden main rotor blades

The main rotor design in figure 2 was realized with Microsoft word 2016.

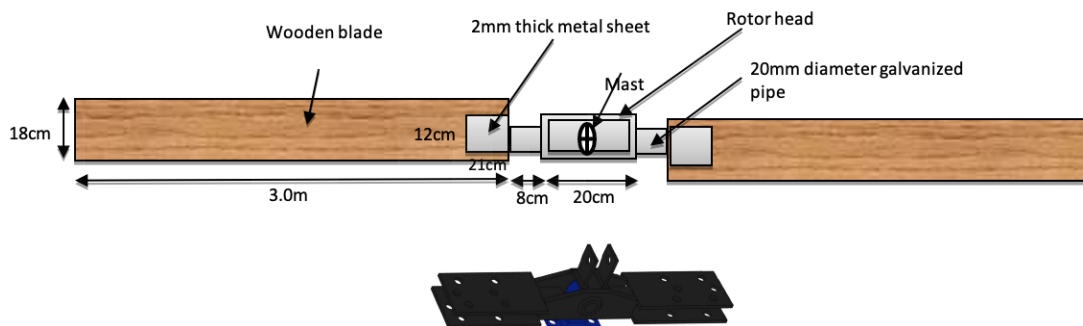
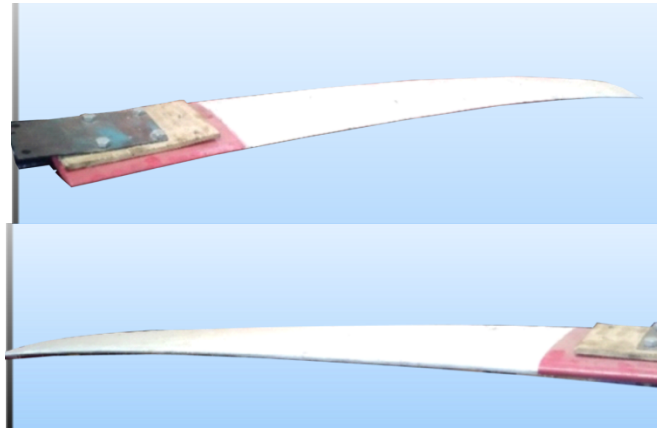


Figure 2: Homemade wooden main rotor blades design



A (a wooden rotor blades)



B (b Rotor blades made of aluminum sheets)

Figure 3: Realized homemade main rotor blades.



Figure 4: Realized and mounted main rotor blades.

The role of the main rotor is realized in figures 3 and 4 to generate the lift force that carries the aircraft's weight. It enables the helicopter to be suspended in the air and provides the control that allows it to follow a prescribed trajectory in the various spatial directions by changing altitude and executing turns. It transfers prevailing aerodynamic forces and moments from the rotating blades to the non-rotating frame (fuselage). The blades are kept in uniform rotational motion (constant speed), by a shaft torque from the engine. A common design solution adopted in the

development of the helicopter is to use hinges at the blades roots that allow free motion of the blade normal to and in the plane of the disc. The most common of these hinges is the flap hinge which allows the blade to flap, that is, to move in a plane containing the blade and the shaft, of the disc plane, about either the actual flap hinge or, in some other cases, the flap hinge is substituted by a region of structural flexibility at the root of the blade. The flap hinge is more frequently designed to be a short distance from the centre line. This is termed an "offset" (eR), and it offers the designer a number of important advantages. A blade which is free to flap, experiences large coriolis moments in the plane of rotation, and a further hinge (called lag) is provided to relieve these moments. This degree of freedom produces blade motion on the same plane as the disc. In presence of aerodynamic loads, this degree of freedom generates the blade's drag force. A blade can also feather around an axis parallel to the blade an. Blade feather motions are necessary to control the aerodynamic lift developed and, in the forward motion of the helicopter, to allow the advancing blade to have a lower angle of incidence than the retreating blade and thereby to balance the lift across the craft. In order to be able to climb up, the feather angle needs to be increased. On the other hand, in order to descend, the blade's feather angle is decreased. Because all blades are acting simultaneously in this case, or collectively, this is known as collective feathering" and allows the rotorcraft to rise/fall vertically. For this control, to achieve forward, backward, and sideways flight, changes of direction are required. The feather on each individual blade is varied at the same selected point on its circular pathway. This is known as cyclic feathering or cyclic control. Blade feather control is achieved through a linkage of the blade to a swashplate [9].

Tail rotor



Figure 4: Realized tail rotor

The tail rotor is mounted perpendicularly to the main rotor, figure 4. It counteracts the torque and the yaw motion naturally produced by the main rotor blades. In accordance to Newton's third law of action and reaction, the fuselage tends to rotate on the opposite direction to the main rotor's blades as a reaction of the torque that appears (Fig. 6).

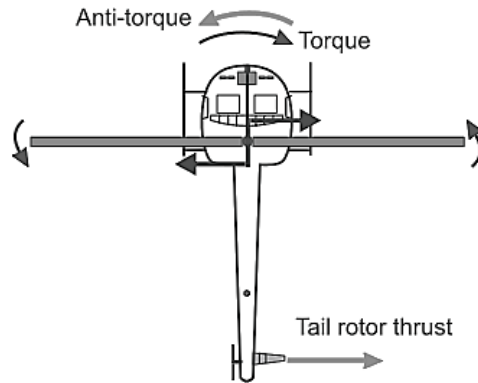


Figure 6: The anti-torque(tail) rotor produces the thrust required to oppose the torque

This torque must be counteracted and/or controlled before any type of flight is possible. Two anti-torque pedals allow the pilot to compensate for torque variance by providing a means of changing pitch (angle of attack) of the tail rotor blades. This provides heading and horizontal directional control during flight. Driven by the main rotor at a constant ratio, the tail rotor produces thrust in a horizontal plane opposite to the torque reaction developed by the main rotor. Since the main rotor torque varies during flight when power changes are made, it is necessary to vary the thrust of the tail rotor. Part of the engine power is required to drive the tail rotor, especially during operations when maximum power is used. Any change in engine power output produces a corresponding change in the torque effect.

Dynamic model description

The parameters used for the design carried out in this work are shown in table 1. For the purpose of dynamic design only, the actions of external forces are not considered, for example: gravity. An unbalance of masses is considered on the main and the tail rotors blades in order to analyse a source of vibrations in the helicopter with an amplitude to be detected in the spectrum, figure 7.



Figure 7: Helicopter realized model

Table 1: Main and tail rotor masses

Parameters	Symbol	Rotors made of aluminum sheet	Wooden rotors
Main Blade one mass	MR_{m1}	2.17kg	3.67kg
Main Blade two mass	MR_{m2}	2.21kg	3.61kg
Tail Blade one mass	TR_{m1}	0.51g	0.51g
Tail Blade two mass	TR_{m2}	0.52g	0.52g
Tail Rotor Speed	TR_s	632rpm	632rpm
Main Rotor Speed	MR_s	551rpm	351rpm

AERODYNAMIC MODEL

Air density

For every flight condition, the air density changes with the height (h), for the lower atmosphere where helicopters fly below 6000 m, the standard value of air density can be approximated as:

$$\rho = \rho_0 e^{-0.0296h/305.6} \quad (1)$$

Where h is expressed in meters and ρ_0 is 1.225kg/m³ (air density at sea level) [10]

Induced velocity

During hover flight, the induced velocity can be obtained as $v_i = v_{io}$, v_{io} is the hover induced velocity, which can be considered constant in hover, the traction force, T , becomes equal to the disc loading (weight of the helicopter), see Figure 8 [10]:

$$v_{io} = \sqrt{\frac{T}{2\rho R^2}} \quad (2)$$

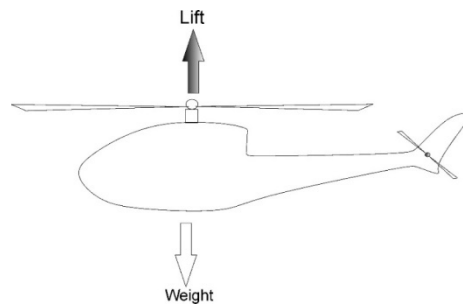


Figure 8: Main forces acting on the helicopter

Blade Element Analysis

Blade element theory forms the basis of most modern analyses in helicopter rotor aerodynamics as it estimates the radial and azimuthal distributions of blade aerodynamic forces (and moments). In addition to this, the rotor performance can be obtained by integrating the sectional airloads at each blade's elements over the length of the blade and averaging the result over a rotor revolution [9]. Figure 9 is a plan view of the rotor disc, viewed from above. The blade radius is R and the tip speed is given by ΩR . An elementary blade section is considered at radius y , of chord length c and spanwise width dy .

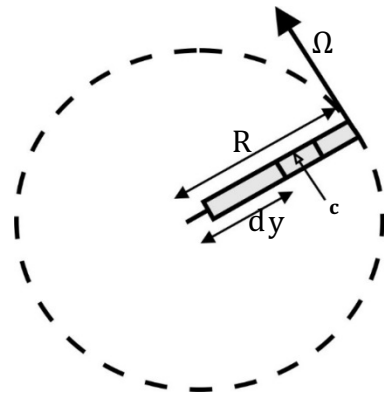


Figure 9: Main rotor disc viewed from above

The velocity components on the blade's section are shown in Figure 4. The flow seen by the section has velocity components Ωy in the disc plane and $(v_i + v_c)$, v_i is the induced velocity and v_c is the upward velocity) perpendicular to it [11]. The resultant local flow velocity at any blade element at a radial distance y from the rotational axis has an out of plane component, figure 10.

$U_p = (v_i + v_c)$ normal to the rotor plane as a result of climb and induced inflow and in plane component $U_T = \Omega y$ parallel to the rotor due to blade rotation, relative to the disc plane. The resultant velocity at the blade element is therefore the composition of both [9]:

$$U = \sqrt{U_p^2 + U_T^2} = [(v_i + v_c)^2 + (\Omega y)^2]^{1/2} \quad (3)$$

The blade's feather angle θ , is imposed by the pilot's collective control input. The angle between the flow direction and the plane of rotation, known as the inflow angle ϕ , is therefore [11]:

$$\tan \phi = \frac{(v_i + v_c)}{\Omega y}$$

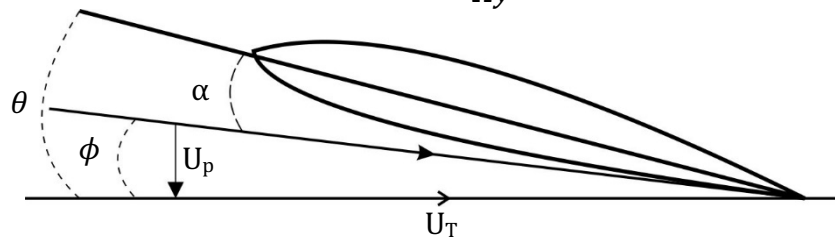


Figure 10: Velocity components U_T and U_P

If the feather angle at the blade element is θ , then the aerodynamic or effective angle of attack is:

$$\alpha = \theta - \phi \quad (4)$$

The resultant incremental lift, dL , and drag dD per unit span on a blade element are:

$$dL = \frac{1}{2} \rho U^2 c C_l dy \quad (5)$$

$$dD = \frac{1}{2} \rho U^2 c C_d dy \tag{6}$$

Where ρ is the air density, C_l and C_d are the lift and drag coefficients, c is the local blade chord. The lift dL and drag dD act perpendicular and parallel respectively to the resultant flow velocity.

Thrust coefficient

The thrust coefficient approximation for hover flight can be written as

$$C_T = \frac{1}{2} \sigma \alpha \left[\frac{1}{3} \theta - \frac{1}{2} \lambda \right] \tag{7}$$

θ is the feathering angle, α is the lift slope, $\lambda = \frac{v_{ih}}{\Omega R}$, v_{ih} is the induced hover velocity, R is the rotor radius and σ is the solidity factor, which for a constant blade chord is given by

$$\sigma = \frac{Nc}{\pi R}$$

N is the number of main rotor blades and c is the blade chord [11].

Kinematic drive diagram of the helicopter

The kinematics diagram of the functioning principle is presented in figure 11.

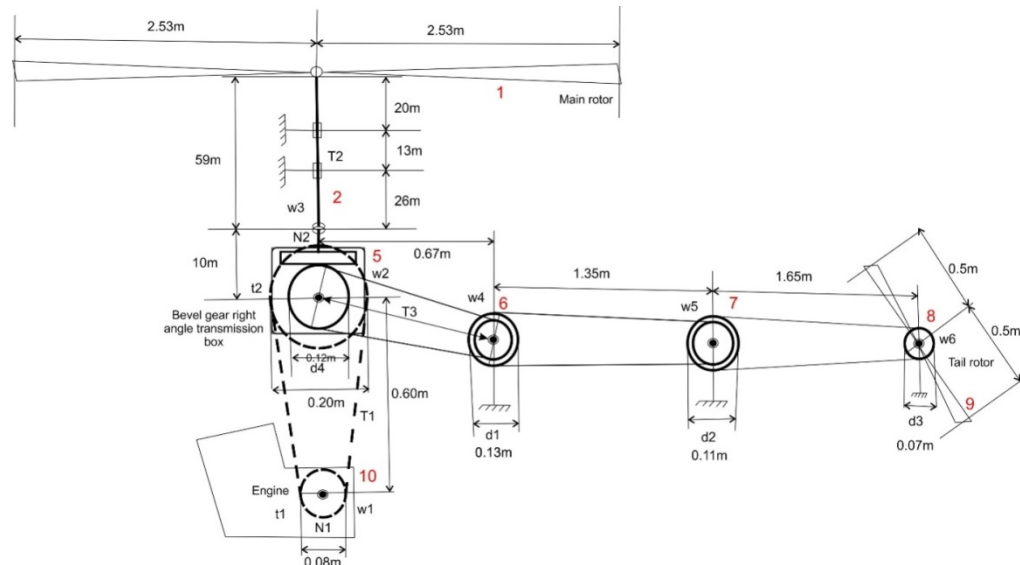


Figure 11: Kinematic diagram of the helicopter.

Data: $d3= d5 =13\text{cm}$, $d4= 12\text{cm}$, $n1, n2= 15$ teeth, $n3= n4= 10$ teeth, The numbers in red indicate the connections of the helicopter system. We notice

As a result, there are 15 links (couplings). Motion transmissions are represented by T_i , where $i =1, 2, 3, 4, 5$.

Degrees of freedom.

The degree of freedom of a system is the number of independent variables required to define the motion or orientation of a rigid body in space (the number of directions or coordinates a body can move). It is used in kinematics to calculate the dynamics of a body.

According to the kinematic diagram of the helicopter as shown in fig 11, we noted 13 couplings, 9 lower pairs, and 2 upper pairs. (Gandhi, 2011) [12]
The total number of degrees of freedom is expressed by the formula,

According to Grubler's Rule

$$F = 3(n - 1) - 2L - h \quad (8)$$

Where

n = Number of coupling (links);

L = Number of lower turning point (revolute joints) (one degree of freedom).

h = Number of upper turning point (half joints) (two degree of freedom).

$n=15$ $L=9$ $h=6$

$$F = 3*(15-1) - 2*9 - 6 = 18$$

Therefore, since $F \geq 1$, the system is a mechanism.

VIBRATIONS ANALYSIS

Analysis of the vibration for the helicopter is a difficult task due to the complexity of the structure, but some accuracy is achievable with modern techniques. This work is carried out by estimating the vibrations transmitted on the fuselage when the aerodynamic model has been implemented as well as a comparison to dynamic vibrations generated, Figure 10. In order to develop the analysis, the following steps : a) detection of vibration signals on the fuselage as a consequence of the aerodynamic load using a vibration sensor and an accelerometer in which the displacements in the x and y axis were measured as a function of time and with unbalance of masses of the rotors were determined using electronic suspending mass scales, b) analysis of the vibrations in the x and y axis with time generated spectrogram with matlab software for identification of the predominant frequencies.

Vibrational transmission

Vibrations appearing on the fuselage's axes X (roll), Y (pitch) and Z (yaw) are studied. X and Y are analyzed and investigated as shown in [7], figure 12k below. aerodynamic model satisfies the following structural characteristics: the flap and lag degrees of freedom do not have springs fitted, although the lag is maintained as a damper.



Figure 12: Vibration detection Arduino module

There is a consequence of the use of a rotating frame of reference that affects vibrational frequencies created on the rotor and transmitted to the fuselage. The frequencies generated by the rotor may include the rotational frequency of the rotor and the external perturbation frequencies [15]. In order to analyze the vibrations appearing on the fuselage, the Short Time Fourier Transform (STFT) was used.

$$S_x(t, \omega) = \int_{-\infty}^{\infty} x(\tau)h(\tau - t)e^{-j\omega \tau} d\tau \quad (9)$$

$X(t)$ is the corresponding signal under study, and $h(t)$ is a finite support window function. The properties of the window function $h(t)$ have a significant effect on the STFT display and should be carefully chosen. For clarity of the view, Matlab simulations were carried out for 50 seconds, although the results plotted in figures 11 and 13 show the first 5 seconds only. The height is $h = 250$ m and the main rotor's collective feather angle is 0.175 rad and the tail rotor's collective feather angle is also 0.175 rad. Figure 13, shows the fuselage's oscillations (vibrations) on the X axis for 5 seconds. Figure 15 depicts the corresponding spectrogram for this simulation in the y-axis. Various predominant frequencies which come from the main rotor loads (approximately 14.4Hz) can be seen on the spectrogram in figures 13 and 14. There is a second predominant frequency (approximately 30.1 Hz). This is twice the flap frequency, and a third predominant frequency is found at around 78.5 Hz.

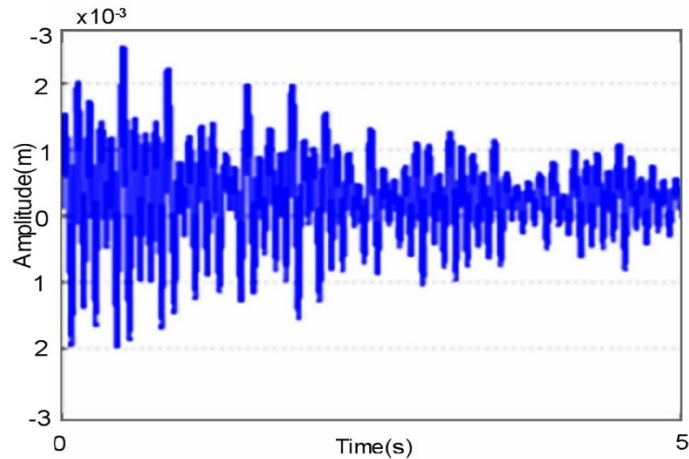


Figure 13: Vibrations on the fuselage x-axis

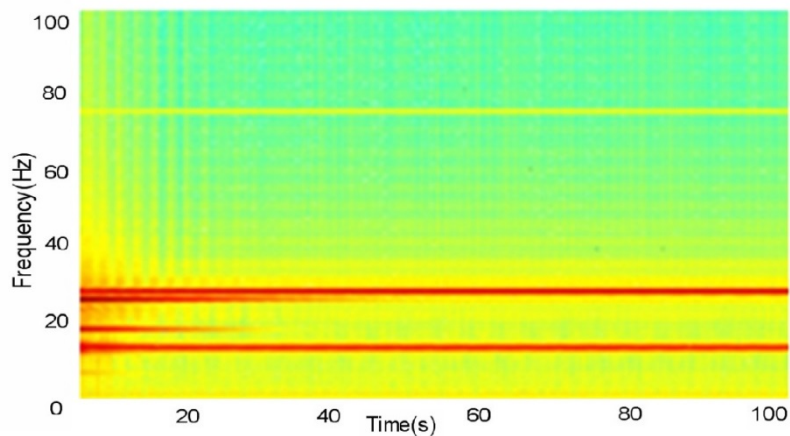


Figure 14: Spectrum on the fuselage x-axis

Similar analysis is carried out for the oscillations appearing on the fuselage's Y axis (see Figure 15). The three predominant frequencies of these vibrations appear in the spectrogram in Figure 16. These are approximately 14.4 Hz which are caused by the main rotor blades' flap, the second frequency is approximately 30.1 Hz, this value is twice the main rotor flap frequency and the third frequency is around 78.5 Hz.

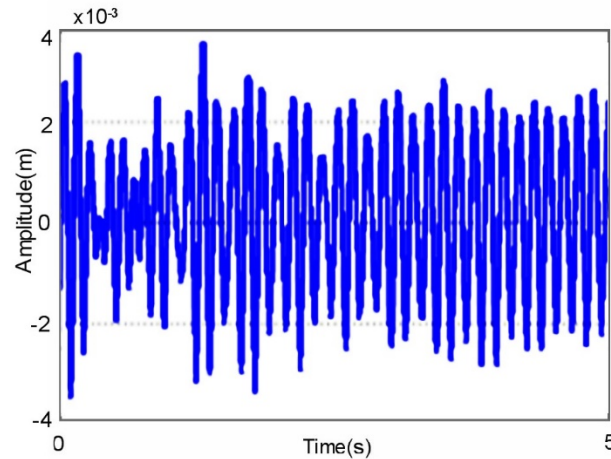


Figure 15: Vibrations on the fuselage y-axis

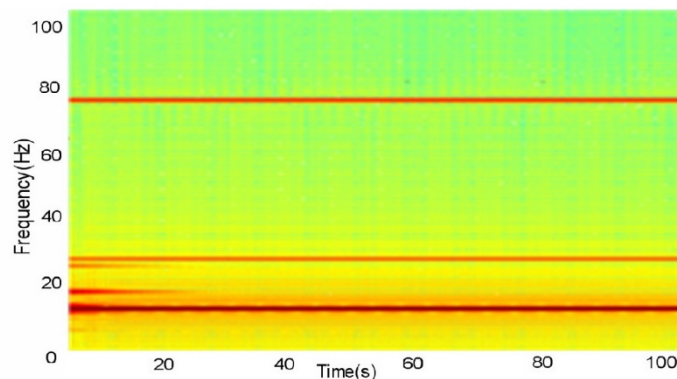


Figure 16: Spectrum on the fuselage y-axis

CONCLUSIONS

The homemade helicopter main rotor blade profile model under study is based on the Sikorsky configuration, the model reproduces the dynamic behaviour of a helicopter, which is capable of transmitting perturbations from the main rotor to the fuselage in form of vibrations. The model has been implemented with used of matlab software for analysis. This work presents a helicopter aerodynamic model in which the blade element theory has been used for the analysis. This is important in order to study and analyze the vibrations appearing in the fuselage as a consequence of aerodynamic load. Various tests under the action of these conditions were carried out in order to study vibrations appearing on the fuselage roll and pitch axes. The fuselage vibration spectrograms were obtained and analyzed using Matlab software's short-time Fourier transform process. When the aerodynamic load was included in the dynamic helicopter model, the obtained results matched those predicted by theoretical approaches. As a consequence, the spectrograms were also studied and showed a reasonable discrepancy according to the expected behaviour introduced by the aerodynamic model.

The homemade helicopter's main rotor blades have been modeled using Matlab. Spectrogram analysis on the fuselage's roll and pitch axes captures transmitted vibrations as a consequence of the aerodynamic load. The results obtained enable the identification of

some predominant frequencies used as reference characteristics for the determination of the stability and the most performant homemade helicopter main rotor blade profile. Compared to the dynamic vibrations obtained with the wooden and aluminum rotor blade profiles, the rotor blade profile with the least predominant frequency is preferred. The homemade helicopter main rotor profile design vibrational analysis was satisfactory. These results are still at an early stage, and the authors expect to develop further analogies with experimental results in future work.

References

- [1] Bramwell, A. R. S., Done, G., Balmford, D. (2001) *Bramwell's Helicopter Dynamics*. Butterworth-Heinemann.
- [2] Castillo-Rivera, S. (2014) "Advanced Modelling of Helicopter Nonlinear Dynamics and Aerodynamics". PhD Thesis. School of Engineering and Mathematical Sciences. City University London.
- [3] Castillo-Rivera, S., Tomas-Rodriguez, M., Marichal-Plasencia, G., N. (2014) "Helicopter Main Rotor Vibration Analysis with Varying Rotating Speed". XXXV Jornadas de Automatica. pp. 34-41. ISBN-13: 978-84-697-5089-6.
- [4] Castillo-Rivera, S., Tomas-Rodriguez, M., Marichal, G., N., López, A. (2013) "Estudio de la interacción del fuselaje y el movimiento de aleteo de las palas del rotor principal en un helicóptero". XXXIV Jornadas de Automatica. pp. 514-521. ISBN 978-84-616-5063-7.
- [5] Ferrer, R., Krysinski, T., Aubourg, P., Bellizi, S. (2001). "New Methods for Rotor Tracking and Balance Tuning and Defect Detection Applied to Eurocopter Products American Helicopter Society" 57th Annual Forum, Washington, DC, May 9-11.
- [6] Johnson, W. (1980) *Helicopter Theory*. Princeton, NJ: Princeton Univ. Press.
- [7] Keysan, O., Ertan, H. Higher Order Rotor Slot Harmonics for Rotor Speed & Position Estimation. 12th International Conference on Optimization of Electrical and Electronic Equipment, OPTIM. 978-1-4244-7040-4.
- [8] Leishman, J. G. (2007) *Principles of Helicopter Aerodynamics*. Cambridge University Press.
- [9] Marichal, G., N., Tomas-Rodriguez, M., Lopez, A., Castillo-Rivera, S., Campoy, P. (2012) "Vibration Reduction for Vision System on Board UAV using a neuro-fuzzy Controller". *Journal of Vibration and Control*. DOI 10.1177/1077546313479632.
- [10] Nguyen K. (1994) "High Harmonic Control Analysis for Vibration Reduction of Helicopter Rotor Systems". NASA Technical Memorandum 103855.
- [11] Seddon, J. (1990) *Basic Helicopter Aerodynamics*. Blackwell Scientific Publications (BSP) Professional Books.
- [12] Sharp, R. S., Evangelou, S., Limebeer, D, J, N.(2005) Multibody aspects of motorcycle modeling with special reference to Autosim, *Advances in Computational Multibody Systems*, J. G. Ambrosio (Ed.), Springer-Verlag, Dordrecht, The Netherlands, 45-68.
- [13] Tomas-Rodriguez M., Sharp R. (2007) "Automated Modeling of Rotorcraft Dynamics with Special Reference to Autosim". *Automation Science and Engineering. CASE 2007. IEEE International Conference*, pp: 974-979.
- [14] Watkinson. J. (2004) *The art of the helicopter*. Elsevier Butterworth-Heinemann.
- [15]Wagtendonk W.J, 2015, *Principles of Helicopter Flight*. Aviation supplies and Academics, Inc Ebook 700 132 nd Place,SE ,ISBN 978-1-61954-299-0.